Fabrication of Syndiotactic Polystyrene Nanocomposites with Exfoliated Clay and Their Properties

Mun Ho Kim,[1] O Ok Park[2,3]

[1]*Reliability Assessment Center for Chemical Materials, Korea Research Institute of Chemical Technology (KRICT), Daejeon 305-600, Republic of Korea*
[2]*Department of Chemical and Biomolecular Engineering (BK 21 Graduate Program), Korea Advanced Institute of Science and Technology (KAIST), Daejeon 305-701, Republic of Korea*
[3]*Department of Energy Systems Engineering, Daegu Gyeongbuk Institute of Science and Technology (DGIST), 50-1, Sang-ri, Hyeongpung-myeon, Dalseong-gun, Daegu 711-873, Republic of Korea*

Received 22 August 2011; accepted 1 December 2011
DOI 10.1002/app.36619
Published online 6 February 2012 in Wiley Online Library (wileyonlinelibrary.com).

ABSTRACT: The fabrication of syndiotactic polystyrene (sPS)/organophilic clay nanocomposite was conducted via melt intercalation process. To obtain sPS nanocomposites with exfoliated clay, the stepwise mixing process using RPS as amorphous styrenic polymer was adopted. Also, organophilic clay modified by cetyl pyridium chloride was used to overcome the thermal instability of commonly used clay and to enhance the compatibility of clay with sPS. We could obtain exfoliated sPS nanocomposites in all compositions without any collapsed clay layers. The microstructures of nanocomposites were confirmed by X-ray diffraction and transmission electron microscopy. The crystallization rate of nanocomposites investigated by differential scanning calorimetry increases with the content of clay, which may be due to the nucleating effect of the clay layer. Nanocomposites exhibited enhanced stiffness relative to the neat polymer.
 J Appl Polym Sci 125: E630–E637, 2012

Key words: syndiotactic polystyrene; clay; nanocomposite; melt intercalation; crystallization

INTRODUCTION

Syndiotactic polystyrene (sPS) is a crystalline polymer with a high melting point (about 270°C), which is polymerized via new metallocene catalysts.[1] It is one of the most attractive polymers as it is based on a commercially available, abundant monomer (styrene), and it give tremendously improved properties over conventional amorphous polystyrene (aPS). The sPS is different from the aPS in that the phenyl rings regularly alternate from side to side with respect to the zigzag polymer chain backbone, and this stereoregular structure allows sPS to crystallize readily. Thus, in addition to the properties of aPS such as low specific gravity, electrical properties, and hydrolytic stability, sPS possesses not only excellent heat and chemical resistance but also dimensional stability. Therefore, sPS is thought to be one of the most promising candidates for a new engineering thermoplastic.[2,3]

It is well known that aPS/clay nanocomposites with different microstructures are easily obtained by the melt intercalation process according to the type of organic modifier in the clay gallery and the polarity of the matrix polymer. Melt mixing or annealing of only two components of aPS and organophilic clay yields nanocomposites with intercalated structure.[4,5] Exfoliated aPS nanocomposites can be obtained by increasing the polarity of the matrix polymer or introducing another polar polymer miscible with aPS.[6,7] However for sPS, it is different. To adopt the melt intercalation process, the processing temperature has to be raised above its melting temperature (270°C). Therefore, the thermal stability issue should be resolved in the first place. On the other hand, the solution blending process at room temperature does not have any thermal stability problems, but two other typical drawbacks can be considered. First, sPS is only soluble to limited solvents, and its cost will be high if both the cost of solvent and the separation cost are included. In addition, organic solvents may cause an environmentally unfriendly situation to take care of. Therefore, it is worth focusing on how sPS nanocomposites can be successfully fabricated via melt processing.

Generally, clay should be modified with alkyl ammonium for the polymer to penetrate easily into the silicate layer because alkyl ammonium makes the hydrophilic silicate surface organophilic. However, it was found out that at around 190°C, the alkyl ammonium part is detached from the organophilic clay so that the gallery spacing is accordingly reduced.[8] To solve this problem, a unique way was developed in the fabrication of sPS nanocomposites: melt intercalation of amorphous styrenic polymers into the gallery

Correspondence to: M. H. Kim (munho@krict.re.kr) or O. Park (ookpark@kaist.ac.kr).

of the organophilic clay followed by blending with sPS.[9–11] This may be called a stepwise mixing process. In this study, the fabrication of sPS nanocomposites with fully exfoliated clay was attempted via stepwise mixing process using oxazoline-styrene copolymer (RPS) as amorphous styrenic polymer. RPS is miscible or partially miscible with sPS without forming domains. Furthermore, it is well known that oxazolin group is reactive toward a number of functional groups, e.g., acids, anhydrides, hydroxyls, and amine.[12]

Besides the polarity of matrix polymer, thermal stability of organophilic clay is essential to fabricate sPS/clay nanocomposite by melt intercalation. In addition, the miscibility between organic modifier and sPS is also a vital factor to disperse clay layers finely into the sPS matrix. Therefore, we decided to fabricate and use organophilic clay modified by cetyl pyridium chloride (CPC) instead of commonly used alkyl ammonium. It is well known that CPC-treated clay is more thermally stable than alkyl ammonium-treated clay. By TGA analysis of the commonly used organophilc clays modified by alkyl ammonium, it was shown that the alkyl ammonium material started to degrade at 150°C and about 70 wt % of the alkyl ammonium material was degraded at 280°C, the melting processing temperature of sPS.[13] This amount of weight loss of organic material brings about the decrease of interlay spacing and deteriorates the compatibility of silicate with polymer. However, CPC-modified clay started to decompose at 250°C, and a considerable portion of the organic material was likely to remain without being degraded at 280°C.[14] In addition, CPC and sPS are miscible with CPC content up to 10 wt % and CPC can act as a plasticizer for sPS, which means that the CPC-modified clay has a good compatibility with sPS.[15] Thus, it is expected that sPS nanocomposites with well-dispersed clay can be obtained because of the high polarity and reactivity of RPS with hydroxyls in clay layer surface, thermal stability of organophilic clay, and miscibility between organic modifier and matrix polymer.

To prove the feasibility of the above fabrication method, organophilic clay modified by CPC was first prepared. The fabrication of sPS nanocomposites via stepwise mixing process was performed using oxazoline–styrene copolymer (RPS) as amorphous styrenic polymer. The microstructure of the fabricated sPS nanocomposites was investigated by X-ray diffraction (XRD) spectra and transmission electron microscope (TEM) image. When considering the properties of sPS nanocomposites, it is important to understand the crystallization behavior and the mechanical properties because sPS is crystalline polymer. Therefore, crystallization behavior of nanocomposites was discussed by differential scanning calorimetric (DSC) analyses, and the mechanical properties of sPS nanocomposites were considered.

EXPERIMENTAL

Materials

The sPS used in this study had weight average molecular weight (M_w) of 256,000 was kindly supplied by Samsung General Chemical Co., and used as received. RPS was the commercial product of Nippon Schokubai Co. with grade name of Epocros RPS-1005 in which 5 wt % oxazolin unit was included. For comparison, atactic polystyrene (aPS) and styrene–maleic anhydride random copolymer (SMA) were also used as amorphous styrenic polymers. aPS (M_w = 412,000) was a commercial grade of Cheil Industry, and SMA (M_w = 224,000) in which the composition of maleic anhydride (MA) was 7 wt % was purchased from Aldrich. Organophilic clay was prepared by ion exchanging sodium montmorillonite (Na^+-MMT) with CPC. Na^+-MMT was supplied by the Southern Clay Co., and the cation exchange capacity (CEC) of this clay is 95 meq/100 g. Cetyl pyridium choloride, a cationic surfactant, was purchased from Aldrich with purity greater than 99%.

Preparation of organophilic clay

The organophilic clay was prepared as follow via ion exchange reaction. A total of 15 g Na-montmorillonite was dispersed into 1500 mL of hot water using homogenizer. A total of 5.814 g CPC (montmorillonte/pyridium salt = 1/1.2 in CEC) was dissolved into hot water. It was poured into the Na-montmorillonite-water solution under vigorous stirring for 30 min to yield with precipitates. The precipitates were collected and washed by hot water three times, and then the precipitates were ground to 50 μm after thoroughly drying in a vacuum oven. This organophilic clay was designed as CPC-MMT.

Preparation of the nanocomposite

sPS-clay nanocomposites were fabricated by stepwise mixing process: melt intercalation of RPS into organophilic clay followed by blending with sPS. Schematic illustration of the fabrication process was shown in Figure 1. At first, a preweighed amount of organophilic clay and RPS were mixed together at room temperature, then melt mixed in a Haake Rheo Mixer 600 at 200°C for 10 min with 50 rpm rotor speed. After completion of mixing, the mixed composite was ejected from the mixing chamber, then cooled and crushed at room temperature. The content of organophilic clay in RPS nanocomposites was 3.3, 10, and 16.7 wt %. sPS nanocomposite was fabricated by blending sPS with the above product in a Haake Rheo Mixer at 280°C for 6 min with 50 rpm rotor speed. The blend ratio of sPS and RPS/

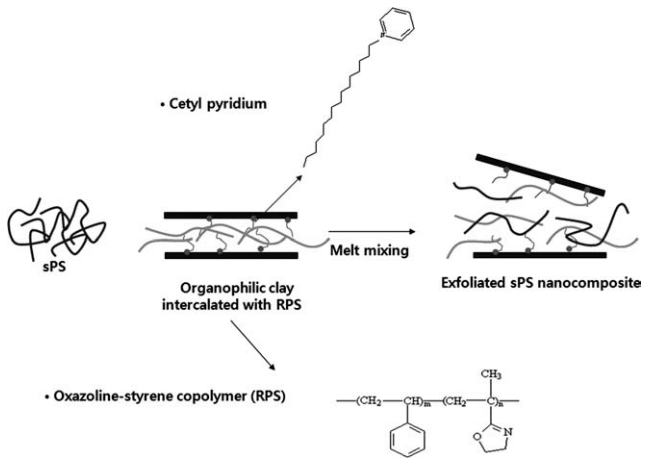

Figure 1 Schematic illustration of the fabrication process of sPS nanocomposites via stepwise mixing process.

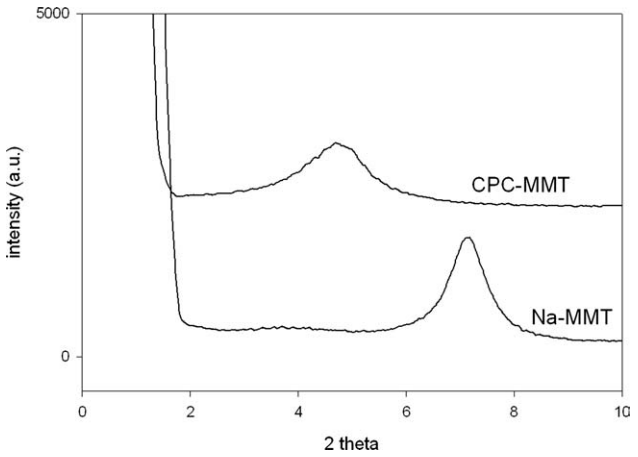

Figure 2 XRD pattern of organophilic clay

organophilic clay was 7 : 3 so that the content of organophilic clay in sPS nanocomposite was 1, 3, and 5 wt %. The compositions of the fabricated nanocomposites are summarized in Table I.

Measurements

The dispersed state of the clay layers in the matrix polymer was evaluated using XRD and TEM. XRD [Rigaku X-ray generator (CuKα radiation with $\lambda = 1.5406$ Å)] spectra were obtained with a 2θ scan range of 0–10° at room temperature. The specimens of the nanocomposite for XRD measurement were obtained in sheet form using a hydraulic press. The dispersion state and layered structure of the clay were observed using TEM (Jeol JEM-2000EX). The specimens were cut into ultrathin slices using a Reichert-Jung Ultracut Microtome at a room temperature without any staining process.

Crystallization and melting behavior of nanocomposites were investigated using DSC (Dupont Ta 2010). The samples were heated to 310°C under a nitrogen atmosphere and held in the melt state for 5 min to eliminate the influence of thermal history. Then, these samples were cooled at different cooling rates of 6, 10, 14, and 20°C/min. The obtained thermograms were analyzed in estimating the crystallization kinetics.

Tensile tests (ASTM D 1708) were performed using a universal tensile machine (Instron UTM). The crosshead speed was 1 mm/min. The flexural modulus (ASTM D 790) was also obtained using UTM. The crosshead speed was 5 mm/min. All specimens for mechanical test were made by injection molding in a minimolder (CSI), and five specimens for each sample were tested and averaged valued were used.

TABLE I
Compositions of Nanocomposites

Sample	SPS (wt %)	RPS (wt %)	Organophilc clay (wt %)	d-spacing (nm)
CPC-MMT	0	0	100	1.88
sPS	100	0	0	–
sPRPS	70	30	0	–
RPS-c3.3	0	96.7	3.3	exfoliation
RPS-c10	0	90	10	3.27 nm
RPS-c16.7	0	83.3	16.7	3.22 nm
sPS-c1	70	29	1	exfoliation
sPS-c3	70	27	3	exfoliation
sPS-c5	70	25	5	exfoliation

RESULTS AND DISCUSSION

Fabrication of sPS nanocomposites by stepwise mixing process

The XRD patterns of the clay are shown in Figure 2. The XRD pattern of sodium montmorillonite shows basal reflections characteristic of $2\theta = 7.0°$. Organophilic clay treated by CPC has the (001) peak at $2\theta = 4.7°$. By Bragg's rule, the *d*-space of clay increases from 1.26 to 1.88 nm. This result indicates that the CPC is indeed intercalated into the layers of clay and the hydrophilic silicate surface changes into an organophilic surface. Thus, hydrophobic polymer chains can be more easily intercalated into the space of the silicate layers.

Microstructure of sPS nanocomposites

The XRD patterns of RPS/CPC-MMT nanocomposites and sPS nanocomposites are shown in Figure 3(A) and (B), respectively. When RPS and organophilic clay were melt-mixed at 200°C as a first step of stepwise mixing method, RPS intercalated nanocomposites structure were obtained. When sPS and RPS/CPC-MMT nanocomposites were mixed at 280°C, we could obtain the exfoliated nanocomposites in all

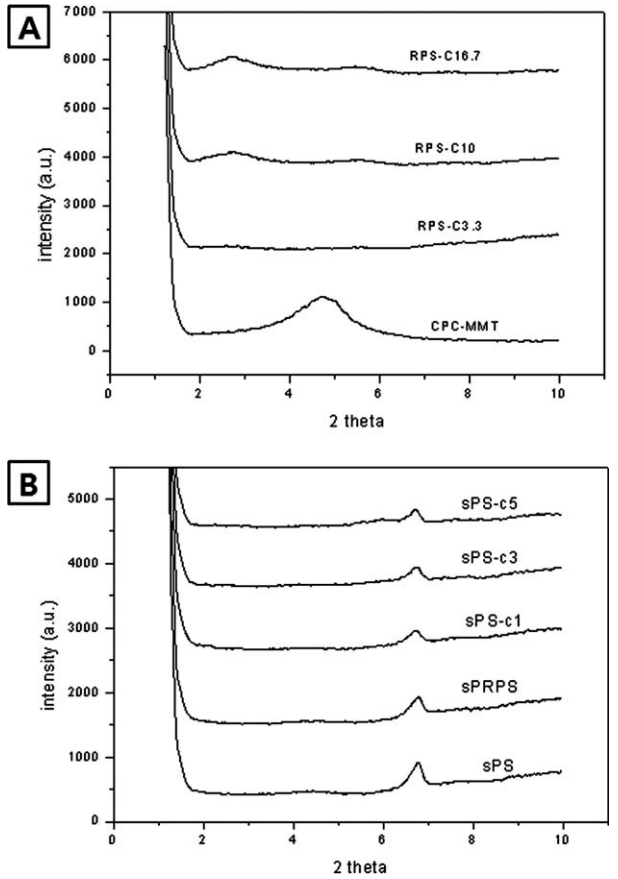

Figure 3 XRD patterns of (A) RPS/CPC-MMT nanocomposites and (B) sPS nanocomposites prepared by stepwise mixing process.

compositions without any collapsed clay layers. The peak around $2\theta = 6.7^\circ$ is the diffraction peak of the hexagonal crystallographic structure of sPS.[16]

It is worthwhile to note microstructural change of the nanocomposite induced by mixing RPS/CPC-MMT nanocomposite with sPS at high temperature. Applied shear stress and heat during the final mixing make it easier for RPS chains to move out from the clay because the RPS chains previously intercalated in the clay gallery become more energetic and have promoted thermal motion. The oxazolin group in OPS has a strong interaction with hydroxyls in clay surface. Thus, the layered structure of clay becomes disordered or exfoliated as RPS and clay layer move together, which is a favorable direction from intercalation to exfoliation without any collapsed clay layers. We believe that thermal stability of CPC-MMT also played an important role in preventing the clay layers from collapsing during melt mixing with sPS at high temperatures.

The microstructures of sPS nanocomposites (clay content of 3 wt %) observed by TEM are shown in Figure 4. For comparison, XRD patterns and TEM images of sPS nanocomposites prepared by the stepwise melt mixing process using aPS and SMA as amorphous styrenic polymers instead of RPS were also shown in Figure 4. In case of aPS, XRD pattern of the (001) peak shifted to $2\theta = 6.24^\circ$, which means the contraction of interlayer spacing and thus the formation of unintercalated structures. TEM image [Fig. 4(B)] showed that unevenly dispersed primary clay particles (tactoids) were observed in the polymer, strongly suggesting an immiscible dispersion.[17] In case of SMA, although XRD pattern indicated nearly no peak, TEM image [Fig. 4(C)] showed that there were intercalated multilayer crystallites present with a few individual layers. On the other hand, TEM image as shown in Figure 4(D) exhibited that individual clay layers were in abundance throughout the polymer, strongly suggesting fully exfoliated morphologies. The dispersion of the clay layers with severely bent structure was also observed in the whole region of TEM image, which means the clay layers were deformed, delaminated, and dispersed finely in the polymer matrix.

On the basis of the results of XRD and TEM experiment, it could be said that sPS nanocomposites with fully exfoliated clay were obtained because of the high reactivity of oxazolin groups in RPS and hydroxyls in clay layer surface.[12] We believe that the miscibility between matrix polymer and organic modifier (CPC) also promoted intermixing of the two chains, and consequently, the clay layers were delaminated more completely.

Crystallization behavior of exfoliated sPS nanocomposites

It is important to investigate the crystallization behavior that occurred during processing as injection molding because sPS is a crystalline polymer. At first, a nonisothermal crystalline study was performed for sPS nanocomposites. It seems desirable to study crystallization behaviors under nonisothermal conditions because isothermal crystallization condition is rarely achievable in practical processing. There have been many suggestions to make a material parameter for directing comparing crystallization rate. Among them, we adopted the crystallization rate parameter (CRP) proposed by Zhang et al.[18] From the nonisothermal crystallization thermograms, the width of the crystallization exothermic peak at half-height divided by the cooling rate yields the isothermal crystallization half-time, $t_{1/2}$, necessary for performing one-half a transition process at a given crystallization temperature. Polymeric material having a slower crystallization rate has a larger $t_{1/2}$. The CRP is determined by the slope in cooling rate versus $1/t_{1/2}$ plot and corresponds to the crystallization rate of the system.

The crystallization temperature (T_c), heat of crystallization (ΔH_c), and half-time of crystallization ($t_{1/}$

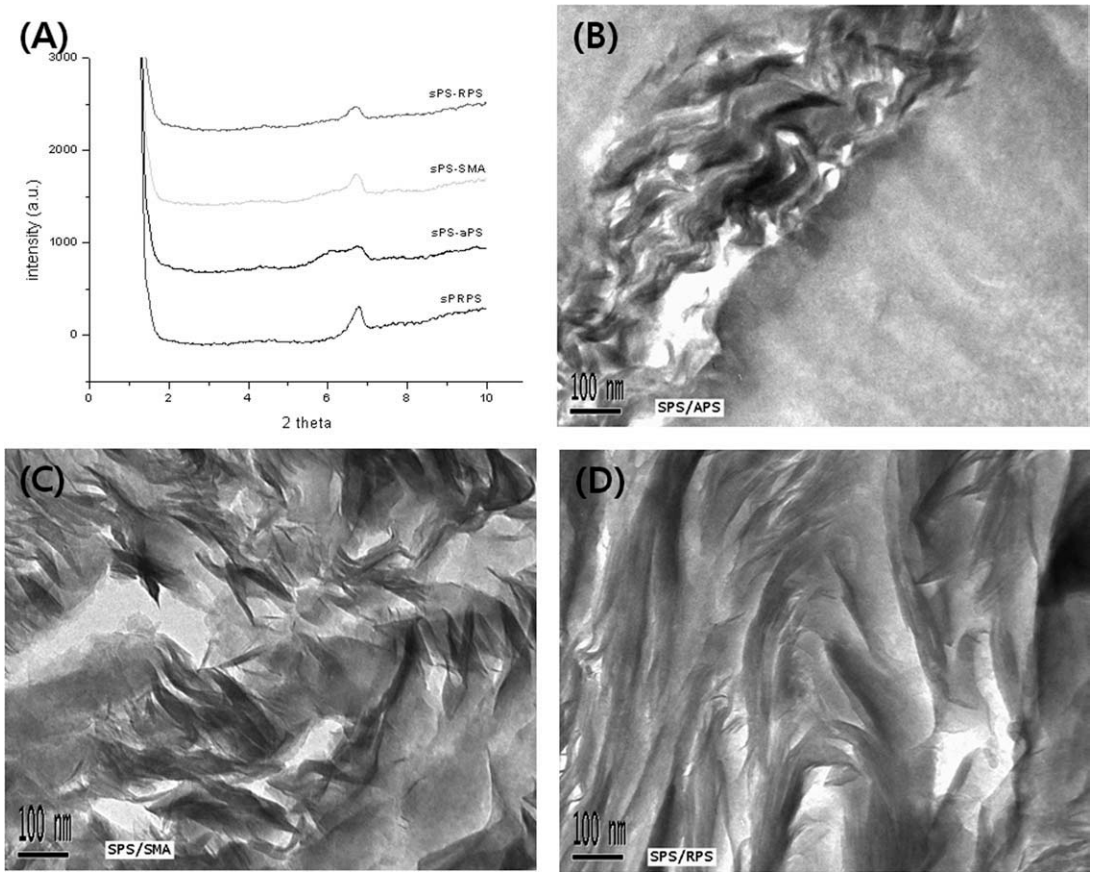

Figure 4 (A) XPD patterns and TEM images of sPS nanocomposites (clay content of 3 wt %) using (B) aPS, (C) SMA, and (D) RPS as amorphous styrenic polymers.

$_2$) obtained from cooling thermograms were summarized in Table II. T_c decreased with the increasing cooling rate, which commonly occurs in polymeric systems due to the difference in time scale between the transformation of polymer chains to crystalline and the cooling rate. When RPS was added to sPS, T_c and ΔH_c decreased because amorphous OPS miscible with sPS interrupted the crystallite formation of sPS. T_c values slightly increase with clay contents, which seemed to be attributed to the nucleation effect of clay. ΔH_c values of sPS nanocomposites are lower those than those of the sPS matrix. This indicates that the crystallite portion was reduced. It seems that the presence of clay hinders the transportation of polymer chains and ultimately crystal growth.

To obtain the CRP, $t_{1/2}$ was measured. At first, the exothermic peak was integrated numerically, and the temperature corresponding to 50% of the peak area ($T_{1/2}$) was found in relative crystallinity (X_c) versus temperature plot. Also, $t_{1/2}$ was obtained by the following equation: $t_{1/2} = (T_i - T_{1/2})/C$. T_i is the initial crystallization temperature, which is the temperature where the thermogram initially departs from the base line. C is the cooling rate. The exo-

TABLE II
Nonisothermal Crystallization Data of sPS Nanocomosites

Sample	Cooling rate (°C/min)	T_c (°C)	ΔH_c (J/g)	$t_{1/2}$ (min)
SPS	6	236.55	21.53	1.2858
	10	232.89	21.17	0.9349
	14	228.58	20.66	0.7174
	20	226.22	20.09	0.5681
sPRPS	6	235.09	17.13	1.4372
	10	229.95	16.47	1.0071
	14	226.02	16.02	0.8201
	20	222.39	15.45	0.6309
sPS-c1	6	234.17	16.46	1.5632
	10	230.55	16.20	1.0896
	14	226.43	15.70	0.8591
	20	221.53	15.27	0.6493
sPS-c3	6	234.66	16.49	1.5827
	10	230.19	16.14	1.0165
	14	225.56	15.68	0.8125
	20	221.49	14.97	0.6341
sPS-c5	6	235.39	16.52	1.5198
	10	228.94	15.53	0.9471
	14	227.19	15.88	0.7857
	20	223.19	15.04	0.5919

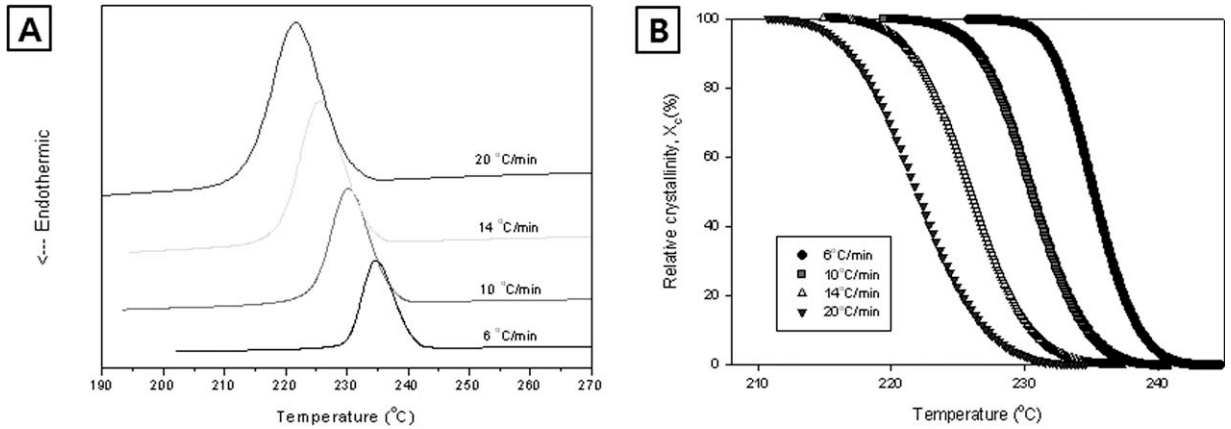

Figure 5 (A) Exotherms of sPS-c3 and (B) their relative crystallinity with different cooling rate.

therms and X_c vs. temperature plot of sPS nanocomposite (clay content of 3 wt %) is displayed in Figure 5 as a typical example. When the reciprocal of $t_{1/2}$ was plotted against the cooling rate, the linear plots were obtained for all samples as shown in Figure 6. The slopes of these plots, i.e., CRP were obtained by linear regression. These CRP values were plotted against the clay content in Figure 7. We could observe that introducing clay followed by a nanoscaled hybrid enhanced the overall crystallization rate. It is believed that this result is attributed to the nucleation effect of clay layer uniformly dispersed in matrix polymer as discussed in T_c. The nucleation effect of clay layers could be found in other polymer/clay nanocomposites such as PET, nylon-6, and PP.[19–21]

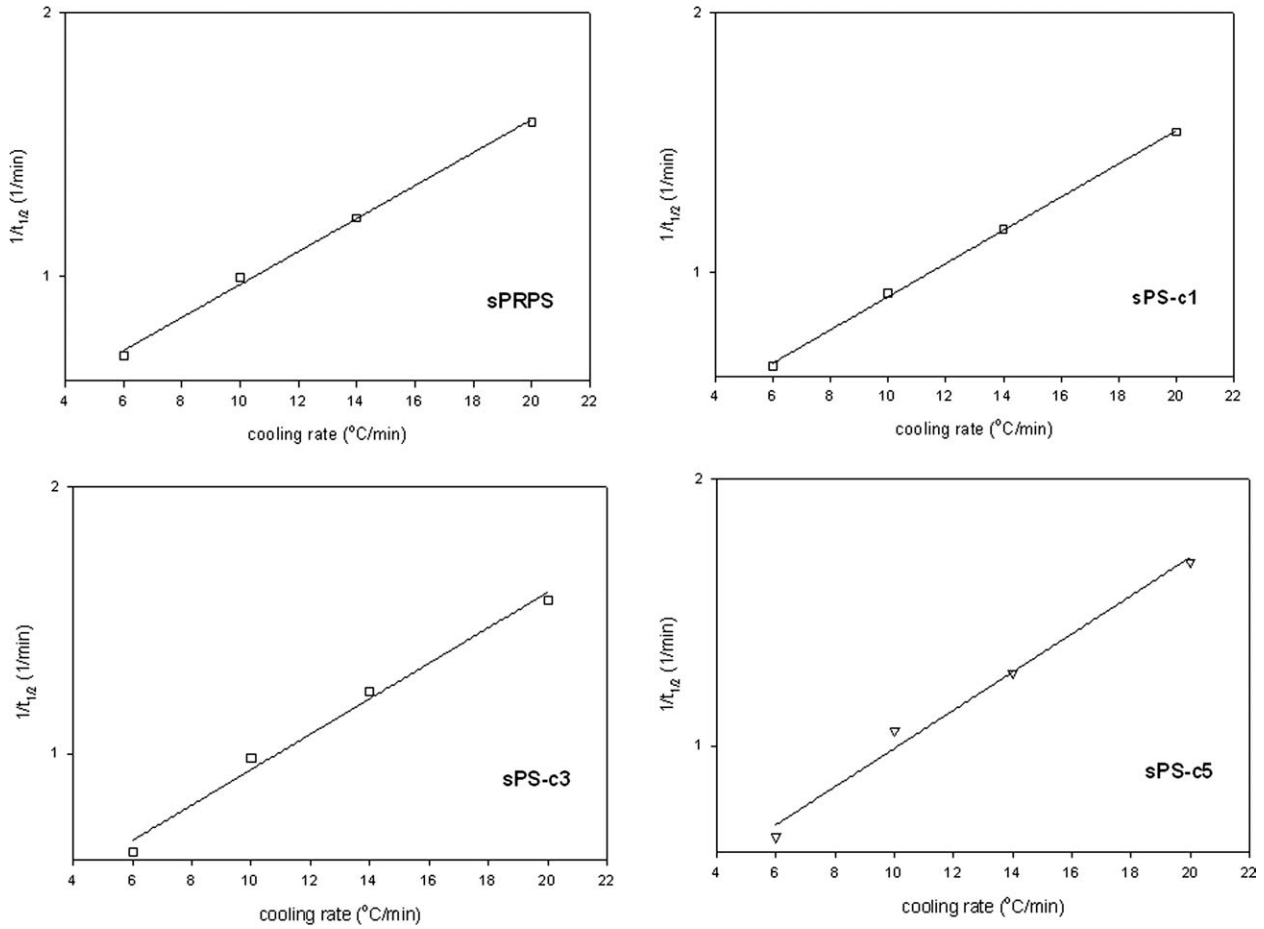

Figure 6 Plot of the reciprocal of half-time of crystallization against cooling rate.

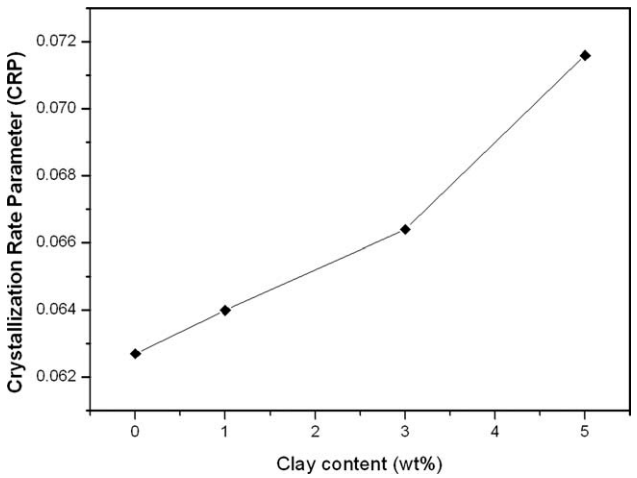

Figure 7 Crystallization rate parameter (CRP) of sPS nanocomposites.

Mechanical properties of exfoliated sPS nanocomposites

Tensile modulus and flexural modulus were measured as mechanical properties. At first, the mechanical properties of the blend of sPS with RPS were measured as reference data. When sPS is blended with RPS, the tensile modulus and flexural modulus show some decrease as shown in Figure 8(A) and (B), respectively. Generally, the crystal structure such as a spherulite in sPS plays an important role in its mechanical properties. This spherulite is known to disrupt by blending with miscible amorphous polymer (RPS), which affects the mechanical properties negatively.[22] From Table II, we could observe that ΔH_c values of sPS nanocomposites are lower those than those of the sPS matrix. Introducing clay followed by a nanoscaled hybrid leads to the reduced ΔH_c values than those of the sPS matrix. The results indicate that the crystallite portion was reduced. It seems that the presence of clay hinders the transportation of polymer chains and ultimately crystal growth, which may affect mechanical properties negatively. However, the tensile modulus of the nanocomposite increases slightly with the increase in clay contents. It is thought that the reinforcement effect of clay in nanoscaled hybrid of polymer and clay is significant enough to surpass the effect of reduced crystallite portion. Flexural modulus also increases with the increase in clay contents in all cases.

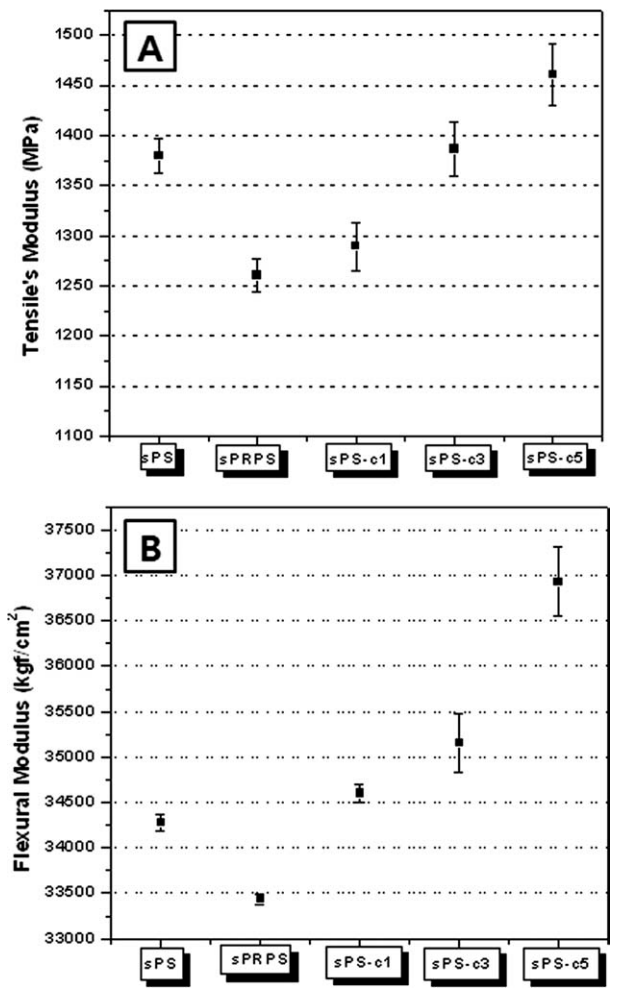

Figure 8 Mechanical properties of sPS nanocomposites: (A) tensile modulus and (B) flexural modulus.

CONCLUSIONS

The fabrication of nanocomposites based on sPS and organophilic clay was investigated. To obtain sPS nanocomposites with exfoliated clay, we adopted the stepwise melt intercalation method using RPS as amorphous styrenic polymer that is miscible with sPS and has a high reactivity with clay layer. And also we used CPC modified clay, which is thermally stable and has a good miscibility with sPS. We could obtain exfoliated sPS nanocomposites in all compositions without any collapsed clay layers. Nanocomposites exhibited an enhanced overall crystallization rate but had less reduced crystallinity than a matrix polymer. Clay layers dispersed in a matrix polymer may serve as a nucleating agent and hinder the crystal growth of polymer chains. Nanocomposites showed increased mechanical properties because of nano-scaled hybrid of polymer and clay.

References

1. Ishihara, N.; Seimiya, T.; Kuramoto, M.; Uoi, M. Macromolecules 1986, 19, 2464
2. Malanga, M. Adv Mater 2000, 12, 1869
3. Schellenberg, J. Syndiotactic Polystyrene: Synthesis, Characterization, Processing, and Applications, Part III; John Wiley: Hoboken, New Jersey, 2009.
4. Vaia, R. A.; Ishii, H.; Giannelis, E. P. Chem Mater 1993, 5, 1694.
5. Sikka, M.; Ceini, L. N.; Ghosh, S. S.; Winey, K. I. J Polymer Sci Part B: Polym Phys 1996, 34, 1443.

6. Vaia, R. A.; Giannelis, E. P. Macromolecules 1997, 30, 8000.
7. Hasegawa, N.; Okamoto, H.; Kawasumi, M.; Usuki, A. J Appl Polym Sci 1999, 74, 3359.
8. Lee, J. W.; Lim, Y. T.; Park, O O. Polym Bull 2000, 45, 191.
9. Park, C. I.; Park, O O., Lim, J. G.; Kim, H. J. Polymer 2001, 42, 7465.
10. Park, C. I.; Kim, M. H., Park, O O. Polymer 2004, 45, 1267.
11. Park, C. I.; Choi, W. M.; Kim, M. H., Park, O O. J Polymer Sci Part B: Polym Phys 2004, 92, 2144.
12. Malaika, A. A. Reactive Modifiers for Polymers; Chapman & Hall: London, UK, 1997; Chapter 4.
13. Kim, M. H.; Park, C. I.; Choi, W. M.; Lee, J. W.; Lim, J. G.; Park, O O.; Kim, J. M. J Appl Polym Sci 2004, 92, 2144
14. Yei, D.-R.; Kuo, S.-W.; Su, Y.-C.; Chang, F.-C. Polymer 2004, 45, 2633
15. Tseng, C.-R.; Wu, J.-Y.; Lee, H.-Y.; Chang, F.-C. Polymer 2001, 42, 10063
16. Lim, R. H.; Woo, E. M. Polymer 2000, 41, 121
17. Morgan, A. B.; Gilman, J. W. J Appl Poly Sci 2003, 87, 1329
18. Zhang, R.; Zheng, H.; Lou, X.; Ma, D. J Appl Polym Sci 1994, 51, 51
19. Ke, Y.; Long, C.; Qi, Z. J Appl Polym Sci 1999, 71, 1139
20. Liu, L.; Qi, Z.; Zhu, X. J Appl Polym Sci 1999, 71, 1133
21. Hambir, S.; Bulakh, N.; Kodgire, P.; Kalgaonkar, R.; Jog, J. P. J Polym Sci Part B: Polym Phys 2011, 39, 446
22. Bonnet, M.; Buhk, M.; Petermann, J. Polym Bull 1999, 42, 353